



Article http://pubs.acs.org/journal/acsodf

# Solution and Solid-State Characterization of PbSe Precursors

Prathamesh B. Vartak, Zhongyong Wang, Thomas L. Groy, Ryan J. Trovitch, and Robert Y. Wang\*



Cite This: ACS Omega 2020, 5, 1949-1955

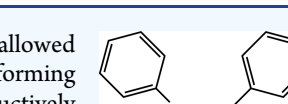


**ACCESS** I

Metrics & More

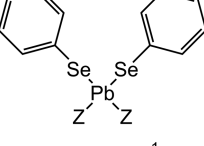


Article Recommendations



Supporting Information

ABSTRACT: The addition of lead to diphenyl diselenide in ethylenediamine (en) or pyridine (py) allowed for the observation of the solvento complexes, (en)Pb(SePh)<sub>2</sub> or (py)<sub>2</sub>Pb(SePh)<sub>2</sub>, respectively. Performing this reaction in dimethyl sulfoxide and subsequent crystallization was found to afford Pb(SePh)<sub>2</sub>. Inductively coupled plasma optical emission spectroscopy revealed a 1:2 lead to selenium ratio for all three complexes. Nuclear magnetic resonance spectroscopy confirms that Pb(SePh), is readily solubilized by ethylenediamine, and electrospray ionization mass spectrometry supports the presence of Pb(SePh)<sub>2</sub> moieties in solution. Single-crystal X-ray diffraction analysis of the pyridine adduct, (py)<sub>2</sub>Pb(SePh)<sub>2</sub>, revealed a seesaw molecular



Z = py, DMSO,  $^{1}/_{2}en$ 

geometry featuring equatorial phenylselenolate ligands. Crystals of Pb(SePh)2 grown from dimethyl sulfoxide revealed onedimensional polymeric chains of Pb(SePh)<sub>2</sub>. We believe that the lead(II) phenylselenolate complexes form via an oxidative addition reaction.

# **■ INTRODUCTION**

Metal phenylchalcogenolates possess rich structural chemistry. Copper(I) phenylselenolate, mercury(II) phenylselenolate, tin(II) phenylchalcogenolates,<sup>3</sup> and lead(II) phenylthiolate<sup>4,5</sup> are known to form one-dimensional (1-D) molecular chains in the solid state, whereas cadmium(II) phenylthiolate and cadmium(II) phenylselenolate are known to form 3D polyadamantanoid cages.<sup>6,7</sup> Copper, mercury, and cadmium phenylchalcogenolates are utilized as starting materials in the synthesis of various cluster compounds.<sup>8–14</sup>

Copper(I) phenylselenolate and tin(IV) phenylselenolate have been utilized as single-source precursors for Cu<sub>2</sub>Se nanocrystals<sup>1</sup> and SnSe nanoparticles, <sup>15</sup> respectively. Moreover, copper(I) phenylthiolate has been considered as an active material for organic electronics, 16 and tin(IV) phenylthiolate has been studied as a CVD precursor to obtain SnS and SnS<sub>2</sub> thin films.<sup>17</sup> Lead phenylselenolate has been explored to a lesser extent, but in principle could function as a precursor for PbSe, which has applications in photodetectors, <sup>18–20</sup> thermoelectrics, <sup>21–26</sup> and photovoltaics. <sup>27–29</sup> We recently discovered that reacting diphenyl diselenide with lead formed a soluble precursor for PbSe. 30 This precursor showed promise for thermoelectric applications, however, its chemical identity was a key unanswered question in that work.

To elucidate the chemical identity of this PbSe precursor, we collected nuclear magnetic resonance (NMR) spectroscopic and electrospray ionization mass spectrometry data on the precursor solution. In addition to performing elemental analyses on the solids collected following solvent removal, single crystals grown separately from pyridine and dimethyl sulfoxide (DMSO) solution were also analyzed by X-ray diffraction. These characterization methods collectively indicate that the chemical identity of the previously described PbSe precursor is solvated lead(II) phenylselenolate.

### RESULTS AND DISCUSSION

Our prior work reported the synthesis of a soluble lead complex that can function as a precursor for PbSe. 30 This precursor was formed by reacting an equimolar amount of diphenyl diselenide with elemental lead in a variety of solvents. We further investigated the thermoelectric properties of PbSe<sub>x</sub>Te<sub>1-x</sub> thin films prepared by mixing PbSe and PbTe precursors. However, the chemical structure of the precursor was not identified at that time. To better understand its composition, we prepared PbSe precursors in ethylenediamine and pyridine and found that these yielded (en)Pb(SePh), (1) and (py)<sub>2</sub>Pb(SePh)<sub>2</sub> (2), respectively. Preparation of the PbSe precursor in DMSO and subsequent crystallization led to the formation of Pb(SePh)<sub>2</sub> (3).

Elemental Analysis of Precursors. We first analyzed the composition of the precursor prepared in an ethylenediamine solution with a 1:1 molar ratio of lead to diphenyl diselenide in accordance with our earlier work. 30 We then dried this reaction mixture in our glovebox to obtain a powder of 1 in 89.6% yield (accounting for incorporation of ethylenediamine from the solvent). Combustion analysis revealed that the carbon wt % is slightly higher, whereas the hydrogen wt % and nitrogen wt % are lower than the expected values for 1 with the atomic composition  $(C_2H_8N_2)Pb(SeC_6H_5)_2$  (refer to 1<sup>a</sup> in Table 1). Inductively coupled plasma optical emission spectroscopy (ICP-OES) on the same powder detected a selenium to lead ratio of 2.08:1 (Table 2). Suspecting that these observations were due to the presence of unreacted diphenyl diselenide in solution, we also performed elemental analysis on 1

Received: November 2, 2019 Accepted: January 8, 2020 Published: January 21, 2020



Table 1. Combustion Analysis of the PbSe Precursor

sample	C (wt %)	H (wt %)	N (wt %)
expected for 1 (C <sub>2</sub> H <sub>8</sub> N <sub>2</sub> )Pb(SeC <sub>6</sub> H <sub>5</sub> ) <sub>2</sub>	29.02	3.13	4.83
1 <sup>a</sup>	29.82	2.93	4
$1^b$	29.1	3.02	4.68
expected for 2 $(C_5H_5N)_2Pb(SeC_6H_5)_2$	39.00	2.98	4.13
2	38.6	2.96	4.03
expected for 3 Pb(SeC <sub>6</sub> H <sub>5</sub> ) <sub>2</sub>	27.75	1.94	
3	27.86	1.76	

<sup>&</sup>lt;sup>a</sup>Synthesized using a 1:1 molar ratio of lead to diphenyl diselenide. <sup>b</sup>Synthesized using a 2:1 molar ratio of lead to diphenyl diselenide.

Table 2. Inductively Coupled Plasma Optical Emission Spectroscopy Analysis on PbSe Precursor

sample	molar ratio, Se:Pb
<b>1</b> <sup>a</sup>	2.08:1
$1^{b}$	2.05:1
3	2.10:1

 $<sup>^</sup>a$ Synthesized using a 1:1 molar ratio of lead to diphenyl diselenide.  $^b$ Synthesized using a 2:1 molar ratio of lead to diphenyl diselenide.

synthesized using a 2:1 molar ratio of lead to diphenyl diselenide. The carbon, hydrogen, and nitrogen weights match those expected for 1 (refer to 1<sup>b</sup> in Table 1). Moreover, ICP-OES on the same powder detected a selenium to lead ratio of 2.05:1, which is closer to the expected value of 2:1 (Table 2).

Repeating these experiments with single crystals of (2) and (3) revealed combustion data close to the expected values for the atomic composition of  $(C_5H_5N)_2Pb(SeC_6H_5)_2$  and  $Pb(SeC_6H_5)_{2t}$  respectively (Table 1). We note that the crystals of 2, obtained from pyridine, changed color from pale yellow to dark orange and lost mass with time. We attribute this color change and mass loss to the loss of pyridine from the crystal structure. This loss of pyridine was also observed upon collecting <sup>1</sup>H NMR data for aged 2 dissolved in DMSO-d<sub>6</sub>. This data shows evidence of free pyridine that has been displaced from aged 2 by the DMSO-d<sub>6</sub> solvent, and the ratio of integrated pyridine peaks to the integrated phenyl peaks is just ~1:6 as opposed to 6:6 (Supporting Information, Figure S8). Consequently, we made sure to perform elemental analysis as soon as the crystals were taken out of the solution. Similar to the ethylenediamine samples, single crystals of (3) were found to feature a selenium to lead ratio of 2.10:1 (Table 2).

Ethylenediamine Complex, (en)Pb(SePh)<sub>2</sub> (1). The ethylenediamine complex of the PbSe precursor was characterized by NMR spectroscopy as well as electrospray ionization mass spectrometry. A combination of <sup>1</sup>H, <sup>13</sup>C, and <sup>77</sup>Se solution NMR spectroscopy confirms that the precursor is solubilized by ethylenediamine. <sup>1</sup>H and <sup>13</sup>C NMR spectroscopy reveal that both phenyl rings of 1 are in the same chemical environment. The <sup>1</sup>H NMR spectrum of this complex shows a distinct splitting pattern of the phenyl rings and two singlets arising from protons of ethylenediamine (Figure 1). Integration of the 1H NMR resonances is consistent with the structural formula (C<sub>2</sub>H<sub>8</sub>N<sub>2</sub>)Pb(SeC<sub>6</sub>H<sub>5</sub>)<sub>2</sub> (Supporting Information, Figure S1). The splitting pattern of the phenyl rings of 1 is comprised of 3 signals (a doublet of doublets and two triplets) corresponding to 3 unique phenyl hydrogen chemical environments. This is in contrast to the splitting pattern of the phenyl rings in diphenyl diselenide that have the signals from

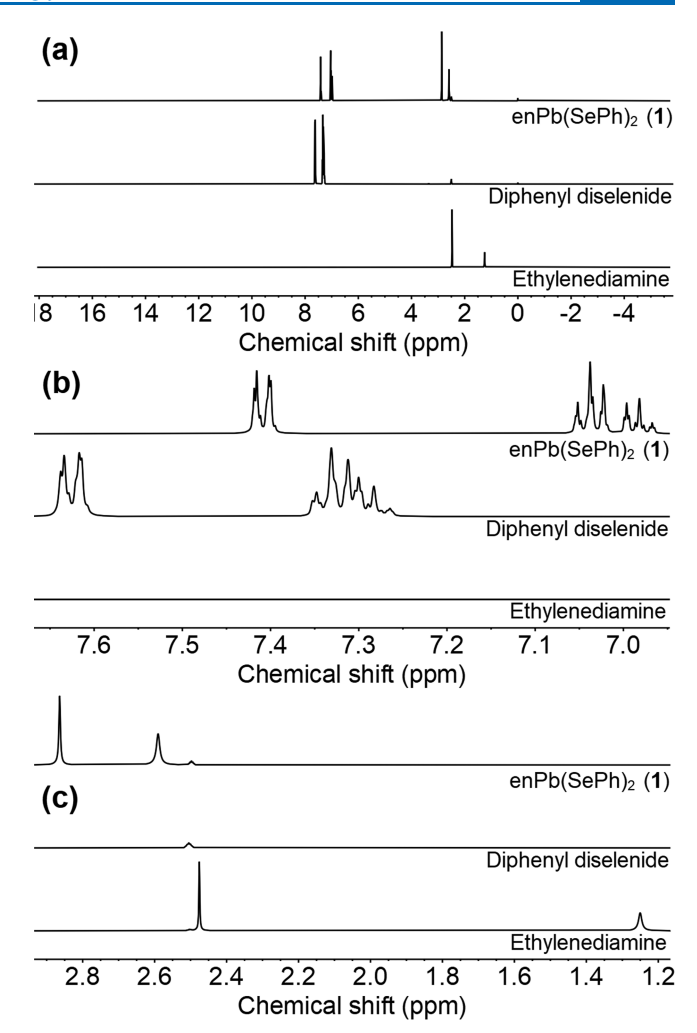


**Figure 1.** Stacked  $^1$ H NMR spectra of (en)Pb(SePh)<sub>2</sub> (1, top), diphenyl diselenide (middle), and ethylenediamine (bottom) in DMSO- $^4$ 6. (a) Complete  $^1$ H NMR spectrum. (b) Magnified region of the same stacked spectra from 6.8 to 7.8 ppm. (c) Magnified region of the same stacked spectra from 1.2 to 2.9 ppm.

the meta- and para-protons merged together to form a multiplet (Figure 1b). Moreover, the resonances for 1 are observed upfield as compared to the proton signals from diphenyl diselenide. This is consistent with the presence of an electropositive Pb atom negating the effect of selenium in deshielding the protons. The resonances of the coordinated ethylenediamine ligand of 1 are observed downfield as compared to signals from pure ethylenediamine (Figure 1c). The 13C NMR spectrum of 1 has 4 signals corresponding to 4 different carbons  $C_v$ ,  $C_o$ ,  $C_m$ , and  $C_p$  present in the phenyl group and a signal corresponding to carbons from ethylenediamine (Figure S2, Supporting Information). Significant differences in chemical shifts were observed in the <sup>13</sup>C NMR spectrum of 1 as compared to the 13C NMR spectra of diphenyl diselenide and ethylenediamine, providing further evidence of complex formation (Figure S3, Supporting Information). A 77 Se NMR resonance was also observed at 188.2 ppm, indicating that selenium is in a single chemical environment. The <sup>77</sup>Se NMR signal of the PbSe precursor appears significantly upfield as compared to the <sup>77</sup>Se NMR signal of diphenyl diselenide, which has a chemical shift of  $\delta$  = 450.9 ppm (Figure S4, Supporting Information). The shielding of selenium atoms (Pauling's electronegativity  $\chi = 2.55$ )

observed in the case of (en)Pb(SePh)<sub>2</sub> as compared to diphenyl diselenide is due to their coordination to an electropositive lead atom (Pauling's electronegativity  $\chi=1.87$ ). This is consistent with the high shielding observed in (Ph)<sub>3</sub>Pb–Se–Pb(Ph)<sub>3</sub> ( $\delta=-454$  ppm), in which selenium is surrounded by two lead atoms.<sup>31</sup> We attempted to collect signals for <sup>207</sup>Pb nuclei in solution for 1 both at room temperature and low temperature (-40 °C), but were unable to obtain a signal. This might be due to an exchange of coordinating ethylenediamine ligands that is faster than the NMR timescale. Nonobservance of the lead signal has been reported for mixed ligand species of PhSe<sup>-1</sup> and PhS<sup>-1</sup> for lead complexes by Dean.<sup>32</sup> Similarly, Rekken et al. did not observe a lead signal for their lithium tristhiolato plumbate (LiPb-(SAr<sup>Me6</sup>)<sub>3</sub>) complex.<sup>33</sup>

Electrospray ionization mass spectrometry on the solution of 1 in ethylenediamine detected the most intense ion cluster at an m/z of 676.9, which corresponds to triligated [PbSe<sub>3</sub>C<sub>18</sub>H<sub>15</sub>]<sup>-1</sup> ions (Figure 2). Other ion clusters were

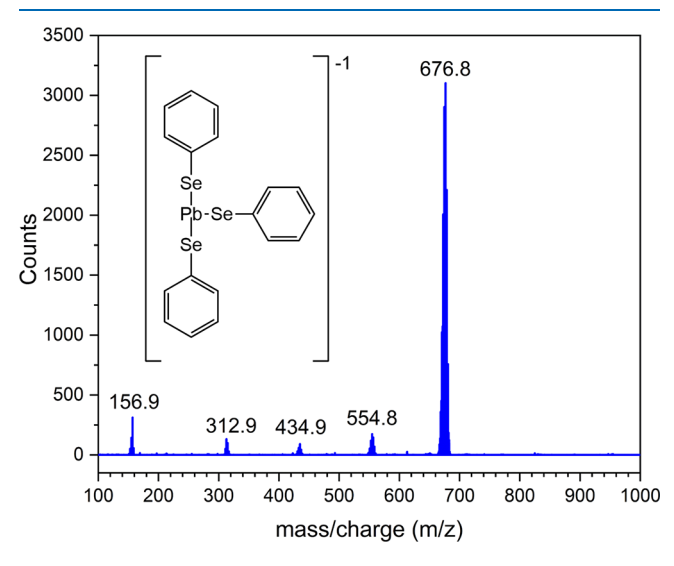


**Figure 2.** Mass spectrum of the PbSe precursor. Ion clusters at m/z 676.8 and 156.9 correspond to  $[PbSe_3C_{18}H_{15}]^{-1}$  ions and  $[SeC_6H_5]^{-1}$  ions.

detected with lower intensities at m/z 156.9, 312.9, 434.9, and 554.8. The ion cluster at m/z 156.9 corresponds to  $[SeC_6H_5]^{-1}$  ions. These ion clusters possess a rich isotopic distribution pattern that originates from the numerous isotopes of lead and selenium. Our ion cluster identification is corroborated by an isotopic distribution comparison between our measured mass spectra and simulated mass spectra (Figure S5, Supporting Information). The ion clusters with low intensities at 312.9, 434.9, and 554.8 remain unidentified. Usually, fragmentation of molecules is observed in mass spectrometry, but on rare occasions, additive processes can occur, especially when the metal ions can coordinate with multiple ligands. The atomic composition of (C<sub>2</sub>H<sub>8</sub>N<sub>2</sub>)Pb-(SeC<sub>6</sub>H<sub>5</sub>)<sub>2</sub> indicated by our elemental analysis data suggests that an additive process occurs to create the triligated  $\begin{array}{c} [PbSe_3C_{18}H_{15}]^{-1} \ ions. \\ We \ hypothesize \ that \ triligated \ [PbSe_3C_{18}H_{15}]^{-1} \ ions \ are \end{array}$ 

We hypothesize that triligated  $[PbSe_3C_{18}H_{15}]^{-1}$  ions are formed during the electrospray ionization process, resulting from the attachment of a  $[SeC_6H_5]^{-1}$  ligand to the neutral  $Pb(SeC_6H_5)_2$  molecule. To confirm this hypothesis, we carried out an additional experiment during which 10 mM of

potassium iodide was added to the solution of 1 in ethylenediamine to assist ionization. We observed that iodide ions ( $I^{-1}$ ) attach to neutral Pb(SeC<sub>6</sub>H<sub>5</sub>)<sub>2</sub> molecules, resulting in detection of an additional ion cluster at m/z 646.7 corresponding to the [PbSe<sub>2</sub>C<sub>12</sub>H<sub>10</sub>I]<sup>-1</sup> ions (Figure S6, Supporting Information). During these experiments with potassium iodide, the triligated  $[PbSe_3C_{18}H_{15}]^{-1}$  ions continued to be observed in greater intensity than the [PbSe<sub>2</sub>C<sub>12</sub>H<sub>10</sub>I]<sup>-1</sup> ions. Lowering of the fragmentor voltage as well as the temperatures of the drying and sheath gas decreased the ratio of triligated  $[PbSe_3C_{18}H_{15}]^{-1}$  ions to  $[PbSe_2C_{12}H_{10}I]^{-1}$  ions, but formation of the triligated  $[PbSe_3C_{18}H_{15}]^{-1}$  ions continued to persist in all cases. This indicates that the neutral molecule  $Pb(SeC_6H_5)_2$  has a greater tendency to ionize itself by utilizing  $[SeC_6H_5]^{-1}$  as a ligand as compared to iodide ions (I<sup>-1</sup>). This occurrence of additive processes in mass spectrometry has also been observed for tin(II) phenylchalcogenolates, resulting in the detection of triligated ions in the corresponding mass spectra.<sup>3</sup>

Pyridine complex, (py)<sub>2</sub>Pb(SePh)<sub>2</sub>. The crystal structure of 2 (deposited with #1955117 in the CCDC database), obtained from single crystals grown from pyridine, is composed of isolated (py)<sub>2</sub>Pb(SePh)<sub>2</sub> molecules (Figure 3).

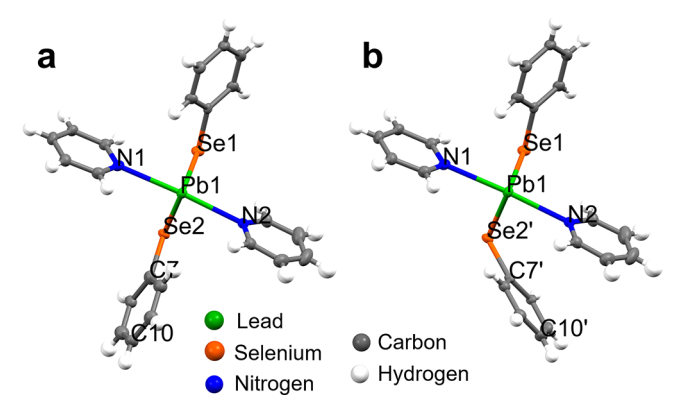


**Figure 3.** Schematic of Pb(SePh)<sub>2</sub>(py)<sub>2</sub> showing disorder in one of the phenylselenolate ligands. (a) Molecule with the occupancy ratio of 0.54 for the disordered ligand indicated by nonprime Se and C atoms. (b) Molecule with the occupancy ratio of 0.46 for the disordered ligand indicated by prime Se and C atoms.

This complex crystallized in a monoclinic space group  $(P12_11)$ , and restraints were required to keep the refinement stable. Importantly, 2 was found to feature a seesaw molecular geometry and axial pyridine ligands with an N(1)-Pb(1)-N(2) angle of 176.1(2)°. In the equatorial plane, one positionally disordered phenylselenolate moiety was identified, with an occupancy ratio of 0.539(1)-0.461(1) for the renderings in Figure 3, respectively. The phenylselenolate ligands are separated by Se(1)-Pb(1)-Se(2) and Se(1)-Pb(1)-Se(2')angles of only 78.14(14) and 84.12(18)°, respectively, which is consistent with the presence of a lone pair of electrons at the third equatorial site. The feature has been noted for the perfluorinated variant of this complex, (py)<sub>2</sub>Pb(SeC<sub>5</sub>F<sub>5</sub>)<sub>2</sub>, <sup>34</sup> as well as Pb(SeCH<sub>2</sub>CH<sub>2</sub>NMe<sub>2</sub>)<sub>2</sub>, 35 which features two chelating 2-(dimethylamino)ethylselenolate ligands. Additional crystallographic data for 2 is presented in Tables S2-S8 of the Supporting Information, and the unit cell packing is shown in Figure S7 of the Supporting Information. Finally, we note that our attempts to collect multinuclear NMR data for 2 dissolved in DMSO-d<sub>6</sub> were unsuccessful due to pyridine ligand substitution by DMSO- $d_6$ . This led to the observation of (DMSO-d<sub>6</sub>)<sub>2</sub>Pb(SePh)<sub>2</sub> (4, refer to "Observation of (DMSO $d_6$ <sub>2</sub>Pb(SePh)<sub>2</sub> (4)" in Experimental Methods and Figures S8 and S9 in the Supporting Information).

One-Dimensional (1-D) Polymeric Chains of Pb-(SePh)<sub>2</sub>. Single-crystal XRD analysis of 3, which was crystallized from DMSO, revealed the presence of 1-D polymeric chains (Figure S10, Supporting Information) consistent with those found in the solid-state structures of other metal phenylchalcogenolates, 1-5 including lead(II) phenylthiolate. 4,5 However, the structure of 3 could not be fully solved due to inversion twinning and disorder (refer to Discussion S1, Supporting Information). Due to the presence of molecular chains in the crystal structure, layering was easily observed for 3 in optical and SEM images (Figure S11, Supporting Information). We also redissolved the single-crystal specimens of 3 in DMSO-d<sub>6</sub> and collected <sup>1</sup>H and <sup>13</sup>C NMR spectra. This led to the observation of 4 (refer to "Observation of (DMSO-d<sub>6</sub>)<sub>2</sub>Pb(SePh)<sub>2</sub> (4)" in Experimental Methods and Figures S12 and S13 in the Supporting Information).

Reaction Mechanism. Our ability to grow crystals of 2 from a pyridine solution indicates that our previously described PbSe precursors are comprised of lead(II) phenylselenolate moieties that coordinate to two functional groups. The solvents used in our prior work<sup>30</sup> can solubilize lead either via nitrogen as in the case of pyridine, ethylenediamine, and butylamine or via oxygen/sulfur as in the case of dimethyl sulfoxide. Similar donor solvent-mediated reactions have been previously observed for elemental zinc and sulfur.<sup>36</sup> The above characterizations identify the PbSe precursor as solubilized lead(II) phenylselenolate and enable us to postulate on the formation mechanism that occurs during the reaction of lead with diphenyl diselenide. We believe that the lead(II) phenylselenolate forms by an oxidative addition reaction during which Pb is oxidized to the +2 oxidation state upon cleavage of the Se-Se bond in diphenyl diselenide. Similar reaction mechanisms have been observed for other metals (e.g., tin, indium, and thallium) when reacted with diphenyl diselenide.37,38

Our synthetic route enables lead(II) phenylselenolate to be used as a solution-processable precursor for PbSe. Our use of ethylenediamine, pyridine, or dimethyl sulfoxide as the solvent yielded solubilized lead(II) phenylselenolate, which has otherwise been reported as insoluble during its synthesis in methanol using benzeneselenol as the selenium source.<sup>3</sup> Lead(II) phenylselenolate synthesized by our route using diphenyl diselenide instead of benzeneselenol is advantageous because of the easy handling of diphenyl diselenide (solid at room temperature) over benzeneselenol, which is an intensely malodorous liquid<sup>39</sup> with high vapor pressure.

# CONCLUSIONS

We identified the molecular structure of a soluble PbSe precursor as solvated lead(II) phenylselenolate and detailed its corresponding solid-state structure. The precursor is synthesized by reacting elemental lead with diphenyl diselenide in ethylenediamine, dimethyl sulfoxide, or pyridine as a solvent. Nuclear magnetic resonance spectroscopy confirms the formation of (en)Pb(SePh)2 for the precursor prepared in ethylenediamine. Single-crystal XRD revealed the molecular structure as (py)<sub>2</sub>Pb(SePh)<sub>2</sub> for a crystal grown from pyridine, whereas 1-D polymeric chains of Pb(SePh)<sub>2</sub> were observed in

crystals grown from dimethyl sulfoxide. We believe that lead(II) phenylselenolate forms via an oxidative addition reaction.

### EXPERIMENTAL METHODS

**PbSe Precursor Synthesis.** The PbSe precursor solution can be synthesized by mixing equimolar amounts of lead and diphenyl diselenide in ethylenediamine, pyridine, or dimethyl sulfoxide as reported previously.<sup>30</sup> In this work, a 2:1 molar ratio of lead to diphenyl diselenide was utilized to ensure that the diphenyl diselenide had reacted completely and thus eliminated the possibility of solubilized diphenyl diselenide in the precursor solution. All syntheses were conducted in a nitrogen-filled glovebox.

Preparation of (en)Pb(SePh)<sub>2</sub> (1). For synthesis using a 2:1 molar ratio of lead to diphenyl diselenide, 0.265 g of lead (1.28 mmol) and 0.200 g of diphenyl diselenide (0.64 mmol) were added to 2 mL of ethylenediamine. The resulting mixture was stirred for 24 h and then filtered using a PTFE filter with a pore size of 0.45  $\mu m$  and a diameter of 25 mm. Subsequent drying afforded 0.310 g of 1. Lowering the amount of lead to 0.133 g (0.64 mmol) and using a 13 mm diameter filter afforded a similar product amount of 0.334 g of 1. <sup>1</sup>H NMR (500 MHz, DMSO- $d_6$ ):  $\delta$  7.41 (dd, 4 H, I = 7.0 and 1.2 Hz; phenyl), 7.04 (pseudo-t, 4 H, J = 7.2 Hz; phenyl), 6.98 (t, 2 H, J = 7.2 Hz; phenyl), 2.86 (s, 4 H; en), 2.59 (s, 4 H; en). <sup>13</sup>C NMR (126 MHz, DMSO- $d_6$ ):  $\delta$  135.4 (phenyl), 133.8 (phenyl), 127.9 (phenyl), 123.9 (phenyl), 43.1 (CH<sub>2</sub>). <sup>77</sup>Se NMR (76.2 MHz, DMSO- $d_6$ ):  $\delta$  188.2. <sup>207</sup>Pb NMR resonances were not observed at room temperature or at low temperature (−40 °C).

Preparation of (py)<sub>2</sub>Pb(SePh)<sub>2</sub> (2) and Subsequent **Crystallization.** We mixed 0.530 g of lead (2.56 mmol) and 0.400 g of diphenyl diselenide (1.28 mmol) in 4 mL of pyridine. The resulting mixture was stirred for 24 h and then filtered using a PTFE filter with a pore size of 0.45  $\mu$ m and a diameter of 25 mm. Single crystals of 2 were obtained by transferring this reaction solution into a 20 mL glass vial and slowly evaporating the pyridine solvent in a nitrogen-filled glovebox. This slow evaporation was done by sealing the top of the vial with a paraffin film and piercing it with a few small holes. After approximately 5 days, clear pale-yellow block-like crystals of 2 were obtained.

Preparation of Pb(SePh)<sub>2</sub> (3) and Subsequent **Crystallization.** We mixed 0.265 g of lead (1.28 mmol) and 0.200 g of diphenyl diselenide (0.64 mmol) in 2 mL of DMSO. The resulting mixture was stirred for 24 h and then filtered using a PTFE filter with a pore size of 0.45  $\mu$ m and a diameter of 25 mm. Single-crystal specimens of 3 were obtained by transferring this reaction solution into a 20 mL glass vial and evaporating the DMSO solvent in a nitrogen-filled glovebox. This evaporation was done by sealing the top of the vial with a paraffin film and piercing it with a few small holes. After approximately 7 days, clear light orange-yellow rectangular parallelepipedal crystals of 3 precipitated from the solution.

Observation of  $(DMSO-d_6)_2Pb(SePh)_2$  (4). Complex 4 can be observed by dissolving 3 in DMSO-d<sub>6</sub>. <sup>1</sup>H NMR (500 MHz, DMSO- $d_6$ ): 7.43 (d, 4 H, J = 6.9 Hz; phenyl), 7.12 (t, 4 H, J = 7.4 Hz; phenyl), 7.03 (t, 2 H, J = 7.3 Hz; phenyl), 3.33 (impurity - H<sub>2</sub>O), 2.54 (impurity - dimethyl sulfoxide). <sup>13</sup>C NMR (126 MHz, DMSO-*d*<sub>6</sub>): 135.4 (phenyl), 132.2 (phenyl), 128.1 (phenyl), 124.4 (phenyl), 40.4 (impurity – dimethyl sulfoxide). Complex 4 can also be observed when 2 is dissolved in DMSO- $d_6$ ; pyridine ligand substitution by DMSO is evidenced by observation of free pyridine in the  $^1H$  NMR spectrum.  $^1H$  NMR (500 MHz, DMSO- $d_6$ ): 8.60–8.55 (m; free pyridine), 7.78 (tt, J=7.6 and 1.9 Hz; free pyridine), 7.43 (d, 4 H, J=6.6 Hz; phenyl), 7.40–7.36 (m; free pyridine), 7.11 (t, 4 H, J=7.5 Hz; phenyl), 7.02 (t, 2 H, J=7.3 Hz; phenyl), 3.33 (impurity –  $H_2O$ ).  $^{13}C$  NMR (126 MHz, DMSO- $d_6$ ): 149.6 (free pyridine), 136.1 (free pyridine), 135.5 (phenyl), 132.2 (phenyl), 128.1 (phenyl), 124.4 (phenyl), 123.9 (free pyridine).

Inductively Coupled Plasma Optical Emission Spectroscopy (ICP-OES). ICP-OES measurements were conducted using a Thermo iCAP6300. The sample was prepared by drying the PbSe precursor solution under vacuum for 2 h. Approximately, 15 mg of 1 was then dissolved in 3 mL of nanopure water and 5 mL of trace metal grade nitric acid. The solution was then diluted by a factor of 100 with nanopure water to ensure that the acid concentration was compatible with the instrument. Similarly, 3 mg of the single-crystal specimens of 3 were dissolved in 1 mL of nanopure water and 2 mL of trace metal grade nitric acid. Dilution by a factor of 100 with nanopure water was carried out for this single-crystal sample as well.

**Combustion Analysis.** The carbon, hydrogen, and nitrogen chemical composition of the products was analyzed using a PE 2400 elemental analyzer. Approximately, 3 mg of 1, 2, and 3 were weighed in a tin cup and then subjected to flash combustion. The instrument's combustion and reduction zones were 980 and 640 °C, respectively. The resulting gases were separated in a gas chromatography column and analyzed using a thermal conductivity detector to quantify the carbon, hydrogen, and nitrogen content. Blank runs were performed after each run to ensure complete combustion of the sample.

Nuclear Magnetic Resonance (NMR) Spectroscopy. <sup>1</sup>H and <sup>13</sup>C NMR measurements were conducted on 1, aged 2, and 3 dissolved in DMSO- $d_6$  at a concentration of 9.5, 9, and 0.6 wt %, respectively. The <sup>1</sup>H and <sup>13</sup>C NMR spectra were collected on a Bruker Avance NEO 500 MHz NMR spectrometer. <sup>1</sup>H spectra were collected with a sweep width of 11 904.8 Hz; a relaxation delay of 5 s and 32 signal averages and referenced internally to the chemical shift of the tetramethylsilane. <sup>13</sup>C spectra were collected with a sweep width of 34 246.6 Hz, a relaxation delay of 2 s, and 256 signal averages and referenced to the chemical shift of the solvent, DMSO-d<sub>6</sub> (39.5 ppm). <sup>77</sup>Se NMR measurements were conducted using a Varian VNMRS 400 MHz NMR spectrometer on 1 dissolved in DMSO- $d_6$  at a concentration of 9.5 wt %. <sup>77</sup>Se NMR spectra were collected with a sweep width of 37 878.8 Hz, a relaxation delay of 6 s, and 48 signal averages. A 0.5 M solution of dimethyl diselenide in CDCl<sub>3</sub> was used as an external chemical shift reference (269 ppm).<sup>40</sup> Moreover, 77Se NMR measurements were conducted on diphenyl diselenide dissolved in DMSO-d<sub>6</sub> at a concentration of 10 wt %.

Mass Spectrometry. Electrospray ionization mass spectrometry was performed using an Agilent 6530 quadrupole time of flight mass spectrometer operated in negative ion detection mode. The glass capillary was subjected to a voltage of 3500 V. The temperature and the flow rate of the drying and sheath gases were maintained at 120 °C and 12 L/min, respectively. The nebulizer pressure was 60 psig, and the fragmentor voltage was 175 V. The ethylenediamine solution of 1 was diluted to a concentration of ∼2 mg/mL and then

further diluted to a concentration  $\sim 1$  mg/mL using methanol. Approximately, 100  $\mu$ L of the sample solution was directly infused into the instrument using a syringe pump at a flow rate of  $\sim 100~\mu$ L/min. The numerous isotopes of Pb and Se yielded rich isotopic distributions in the spectral patterns. All m/z values given in the text correspond to the most abundant peak of the respective isotopic distributions.

Scanning Electron Microscopy and Optical Microscopy. We observed the single-crystal specimen of 2 and 3 using a Zeiss Axio Zoom.V16 optical microscope at a low magnification of 25× as well as using an Amray 1910 field emission SEM at a magnification of 1000× and 5000×.

Single-Crystal X-ray Diffraction. A single-crystal specimen of 2 of approximate dimensions 0.12 mm × 0.18 mm × 0.22 mm was used for the X-ray crystallographic analysis using a Bruker Smart APEX single-crystal diffractometer with Mo Klpharadiation. The specimen was mounted on the tip of a glass fiber using a small amount of Apiezon type N grease. The temperature of the crystal was maintained at 123 K using an Oxford Cryosystems Cryostream 600 low-temperature device. The detector was maintained at 5 cm from the crystal. Data was collected in 3 sets by setting  $\varphi$  angles for each set ( $\varphi = 0$ , 120, and 240°) and varying  $\omega$  (326–144° in –0.5° wide scans per frame at each  $\varphi$  angle),  $2\theta$  (-34°) and  $\chi$  (54.8°). A total of 1092 frames were collected at a rate of 30 s per frame. The frames were integrated with the Bruker SAINT software package using a narrow-frame algorithm. 41 Data were corrected for absorption effects using the multiscan method (SA-DABS).41 The structure was solved by direct methods using the SHELXTL XT-2014/4 program<sup>42</sup> and was refined by a full-matrix least-squares method on  $F^2$  values using the SHELXL-2014/7 program.<sup>43</sup> The crystal data and structure refinement details for 2 are summarized in Table 3, and additional details of data collection and refinement are included in Table S1, Supporting Information. A single-crystal specimen of 3 of approximate dimensions 0.06 mm × 0.13 mm × 0.37 mm was analyzed in a similar manner.

Table 3. Crystal Data and Structure Refinement for 2

chemical formula	$C_{22}H_{20}N_2PbSe_2$		
formula weight	677.51 g/mol		
wavelength	0.71073 Å		
crystal system	monoclinic		
space group	$P12_{1}1$		
unit cell dimensions	a = 5.4824(2)  Å		
	b = 9.0496(3)  Å		
	c = 21.3585(8)  Å		
	$\alpha = 90^{\circ}$		
	$\beta = 93.8688(5)^{\circ}$		
	$\gamma = 90^{\circ}$		
volume	1057.26(7) Å <sup>3</sup>		
Z	2		
density (calculated)	$2.128 \text{ g/cm}^3$		
absorption coefficient	11.430 mm <sup>-1</sup>		
reflections collected	8938		
independent reflections	$3871 \left[ R_{\rm int} = 0.0252 \right]$		
goodness-of-fit on $F^2$	1.032		
final R indices $(I > 2\sigma(I))$	R1 = 0.0245		
	wR2 = 0.0585		
R indices (all data)	R1 = 0.0257		
	wR2 = 0.0592		

# ASSOCIATED CONTENT

# Supporting Information

The Supporting Information is available free of charge at https://pubs.acs.org/doi/10.1021/acsomega.9b03715.

Additional information regarding NMR spectra, mass spectra, and crystallographic data; Figures S1–S13, Discussion S1, and Tables S1–S8 (PDF)
PbSe pyridine 2019 07 25 Final (CIF)

# **Accession Codes**

CCDC #1955117 contains the supplementary crystallographic data for this paper. These data can be obtained free of charge via www.ccdc.cam.ac.uk/data\_request/cif, by emailing data\_request@ccdc.cam.ac.uk, or by contacting The Cambridge Crystallographic Data Centre, 12 Union Road, Cambridge CB21EZ, UK; Fax: +44 1223 336033.

## AUTHOR INFORMATION

# **Corresponding Author**

Robert Y. Wang — Arizona State University, Tempe, Arizona; orcid.org/0000-0002-3888-6906; Email: rywang@asu.edu

### Other Authors

**Prathamesh B. Vartak** – Arizona State University, Tempe, Arizona

**Zhongyong Wang** – Arizona State University, Tempe, Arizona

**Thomas L. Groy** — Arizona State University, Tempe, Arizona

Ryan J. Trovitch — Arizona State University, Tempe, Arizona; orcid.org/0000-0003-4935-6780

Complete contact information is available at: https://pubs.acs.org/10.1021/acsomega.9b03715

#### **Author Contributions**

The manuscript was written through the contributions of all authors. All authors have given approval to the final version of the manuscript.

## Funding

This work was supported by the National Science Foundation through award number DMR-1506829.

#### Notes

The authors declare no competing financial interest.

### ACKNOWLEDGMENTS

We acknowledge the use of facilities within Goldwater Environmental Laboratory, Mass Spectrometry Facility, Magnetic Resonance Research Center, and the Eyring Materials Center (supported in part by NNCI-ECCS-1542160) at Arizona State University. We also thank Brian Cherry, Daniel Brune, Megan Maurer, Jia Fan, Natasha Zolotova, and Cathy Kochert for insightful discussions.

## REFERENCES

(1) Low, K. H.; Li, C.; Roy, V. A. L.; Chui, S. S.; Chan, S. L.; Che, C. Homoleptic Copper(I) Phenylselenolate Polymer as a Single-Source Precursor for Cu<sub>2</sub>Se Nanocrystals. Structure, Photoluminescence and Application in Field-Effect Transistor. *Chem. Sci.* **2010**, *1*, 515–518. (2) Lang, E. S.; Dias, M. M.; Abram, U.; Vázquez-López, E. M. Benzeneselenolates of Mercury(II). Crystal and Molecular Structures

- of  $[Hg(SePh)_2]$  and  $(Bu_4N)[Hg(SePh)_3]$ . Z. Anorg. Allg. Chem. 2000, 626. 784–788.
- (3) Eichhöfer, A.; Jiang, J.; Sommer, H.; Weigend, F.; Fuhr, O.; Fenske, D.; Su, C.; Buth, G. 1-D-Tin(II) Phenylchalcogenolato Complexes [Sn(EPh)<sub>2</sub>] (E = S, Se, Te) Synthesis, Structures, Quantum Chemical Studies and Thermal Behaviour. *Eur. J. Inorg. Chem.* **2010**, 410–418.
- (4) Giffard, M.; Mercier, N.; Gravoueille, B.; Ripaud, E.; Luc, J.; Sahraoui, B. Polymorphism of Lead(II) Benzenethiolate: A Noncentrosymmetric New Allotropic Form of Pb(SPh)<sub>2</sub>. *CrystEngComm* **2008**, *10*, 968–971.
- (5) Rae, A. D.; Craig, D. C.; Dance, I. G.; Scudder, M. L.; Dean, P. A. W.; Kmetic, M. A.; Payne, N. C.; Vittal, J. J. The Pseudo-Symmetric Structure of Pb(SPh)<sub>2</sub>. *Acta Crystallogr., Sect. B: Struct. Sci.* **1997**, *53*, 457–465.
- (6) Craig, D.; Dance, I. G.; Garbutt, R. The Three-Dimensionally Non-Molecular Polyadamantanoid Structure of Cd(SPh)<sub>2</sub>. *Angew. Chem., Int. Ed.* **1986**, 25, 165–166.
- (7) Anjali, K. S.; Vittal, J. J. Polylinked Adamantanoid Structure of Cd(SePh). *Inorg. Chem. Commun.* **2000**, *3*, 708–710.
- (8) Cabral, B. N.; Zawatski, L. E.; Abram, U.; Lang, E. S. Synthesis and Structural Characterization of Copper(I) Phenylselenolate Complexes Stabilized by N,N'-Donor Ligands. *Z. Anorg. Allg. Chem.* **2015**, *641*, 739–743.
- (9) Lang, E. S.; de Oliveira, G. M.; Tirloni, B.; Lago, A. B.; Vazquez-Lopez, E. M. On the Use of Mercury Bis(Phenylselenolate) for the Synthesis of Polymeric Clusters: Synthesis and X-Ray Structural Characterization of  $[Hg_5Cl_3(PhSe)_7]_n$ ,  $[Hg_7Cl_3(PhSe)_{11}]_n$  and  $[Hg_7Br_3(PhSe)_{11}]_n$ . *J. Cluster Sci.* **2009**, 20, 467–479.
- (10) Lago, A. B.; Lang, E. S.; Tirloni, B.; Vázquez-López, E. M. Synthesis and Structural Characterization of a Binary Metal Cluster and a Coordination Polymer Based on the Mercury Bis-(Phenylselenolate) Unit. *Polyhedron* **2012**, *43*, 170–175.
- (11) Lang, E. S.; Back, D. F.; de Oliveira, G. M. Improving the Use of Mercury Bis(Phenyltellurolate) as Efficient Start for the Synthesis of Ternary Clusters and Polymers. *Polyhedron* **2008**, *27*, 3255–3258.
- (12) Stieler, R.; Burrow, R. A.; Piquini, P.; Lang, E. S. Building Hg(II)/Cu(I) Multinuclear Compounds from Mercury Bis (Phenylselenolate). *J. Organomet. Chem.* **2012**, 703, 9–15.
- (13) Lang, E. S.; Burrow, R. A.; Stieler, R.; Villetti, M. A. Cadmium Bis(Phenylselenolate) as a Precursor for the Synthesis of Polymeric  $Cd(\mu$ -Se) Clusters: Crystal and Molecular Structures of  $[Cd_4(SePh)_7(PPh_3)X]_n(X = Cl, Br)$ . J. Organomet. Chem. 2009, 694, 3039–3042.
- (14) Lang, E. S.; Stieler, R.; de Oliveira, G. M. Synthesis, Structural Characterization and Growth Features of Some (Ph)Se-Cd Cluster Compounds (Ph = Phenyl). *Polyhedron* **2010**, 29, 1760–1763.
- (15) Schlecht, S.; Budde, M.; Kienle, L. Nanocrystalline Tin as a Preparative Tool: Synthesis of Unprotected Nanoparticles of SnTe and SnSe and a New Route to (PhSe)<sub>4</sub>Sn. *Inorg. Chem.* **2002**, *41*, 6001–6005.
- (16) Che, C.; Li, C.; Chui, S. S.; Roy, V. A. L.; Low, K. Homoleptic Copper(I) Arylthiolates as a New Class of p-Type Charge Carriers: Structures and Charge Mobility Studies. *Chem. Eur. J.* **2008**, *14*, 2965–2975.
- (17) Barone, G.; Hibbert, T. G.; Mahon, M. F.; Molloy, K. C.; Price, L. S.; Parkin, I. P.; Hardy, A. M. E.; Field, M. N. Deposition of Tin Sulfide Thin Films from Tin(IV) Thiolate Precursors. *J. Mater. Chem.* **2001**, *11*, 464–468.
- (18) Sarasqueta, G.; Choudhury, K. R.; Subbiah, J.; So, F. Organic and Inorganic Blocking Layers for Solution-Processed Colloidal PbSe Nanocrystal Infrared Photodetectors. *Adv. Funct. Mater.* **2011**, *21*, 167–171.
- (19) Martin, J. M.; Hernández, J. L.; Adell, L.; Rodriguez, A.; López, F. Arrays of Thermally Evaporated PbSe Infrared Photodetectors Deposited on Si Substrates Operating at Room Temperature. Semicond. Sci. Technol. 1996, 11, 1740–1744.

- (20) Sarasqueta, G.; Choudhury, K. R.; So, F. Effect of Solvent Treatment on Solution-Processed Colloidal PbSe Nanocrystal Infrared Photodetectors. *Chem. Mater.* **2010**, 22, 3496–3501.
- (21) Gayner, C.; Kar, K. K.; Kim, W. Recent Progress and Futuristic Development of PbSe Thermoelectric Materials and Devices. *Mater. Today Energy* **2018**, *9*, 359–376.
- (22) Wang, H.; Pei, Y.; Lalonde, A. D.; Snyder, G. J. Heavily Doped p-Type PbSe with High Thermoelectric Performance: An Alternative for PbTe. *Adv. Mater.* **2011**, 23, 1366–1370.
- (23) Chen, Z.; Ge, B.; Li, W.; Lin, S.; Shen, J.; Chang, Y.; Hanus, R.; Snyder, G. J.; Pei, Y. Vacancy-Induced Dislocations within Grains for High-Performance PbSe Thermoelectrics. *Nat. Commun.* **2017**, *8*, No. 13828.
- (24) Zhou, C.; Lee, Y. K.; Cha, J.; Yoo, B.; Cho, S. P.; Hyeon, T.; Chung, I. Defect Engineering for High-Performance n-Type PbSe Thermoelectrics. *J. Am. Chem. Soc.* **2018**, *140*, 9282–9290.
- (25) You, L.; Liu, Y.; Li, X.; Nan, P.; Ge, B.; Jiang, Y.; Luo, P.; Pan, S.; Pei, Y.; Zhang, W.; et al. Boosting the Thermoelectric Performance of PbSe through Dynamic Doping and Hierarchical Phonon Scattering. *Energy Environ. Sci.* **2018**, *11*, 1848–1858.
- (26) Qian, X.; Zheng, L.; Xiao, Y.; Chang, C.; Zhao, L. D. Enhancing Thermoelectric Performance of n-Type PbSe: Via Additional Meso-Scale Phonon Scattering. *Inorg. Chem. Front.* **2017**, *4*, 719–726.
- (27) Zhang, J.; Gao, J.; Church, C. P.; Miller, E. M.; Luther, J. M.; Klimov, V. I.; Beard, M. C. PbSe Quantum Dot Solar Cells with More than 6% Efficiency Fabricated in Ambient Atmosphere. *Nano Lett.* **2014**, *14*, 6010–6015.
- (28) Zhang, Z.; Chen, Z.; Zhang, J.; Chen, W.; Yang, J.; Wen, X.; Wang, B.; Kobamoto, N.; Yuan, L.; Stride, J. A.; et al. Significant Improvement in the Performance of PbSe Quantum Dot Solar Cell by Introducing a CsPbBr<sub>3</sub> Perovskite Colloidal Nanocrystal Back Layer. *Adv. Energy Mater.* **2017**, *7*, No. 1601773.
- (29) Davis, N. J. L. K.; Böhm, M. L.; Tabachnyk, M.; Wisnivesky-Rocca-Rivarola, F.; Jellicoe, T. C.; Ducati, C.; Ehrler, B.; Greenham, N. C. Multiple-Exciton Generation in Lead Selenide Nanorod Solar Cells with External Quantum Efficiencies Exceeding 120%. *Nat. Commun.* 2015, 6, No. 8259.
- (30) Wang, Z.; Ma, Y.; Vartak, P. B.; Wang, R. Y. Precursors for PbTe, PbSe, SnTe, and SnSe Synthesized Using Diphenyl Dichalcogenides. *Chem. Commun.* **2018**, *54*, 9055–9058.
- (31) Bahr, S. R.; Boudjouk, P. A Convenient Synthesis of 1,1,1,3,3,3-Hexaphenyldiplumbathiane and 1,1,1,3,3,3-Hexaphenyldiplumbaselenane. *Inorg. Chem.* **1992**, *31*, 4015–4016.
- (32) Arsenault, J. J. I.; Dean, P. A. W. A Preparative and Multinuclear Nuclear Magnetic Resonance Spectroscopic Study of  $As(SPh)_x(SePh)_{3-x}$  (x=0-3),  $Sb(SPh)_x(SePh)_{3-x}$  (x=0-3),  $Bi(SPh)_3$ ,  $Bi(SePh)_3$ ,  $[Sn(SPh)_x(SePh)_{3-x}]^-$  (x=0-3),  $Pb(SePh)_3^-$ , and  $Pb(SPh)_3^-$  and Some Related Thiolatoplubates(II). *Can. J. Chem.* **1983**, *61*, 1516–1523.
- (33) Rekken, B. D.; Brown, T. M.; Olmstead, M. M.; Fettinger, J. C.; Power, P. P. Stable Plumbylene Dichalcogenolate Monomers with Large Differences in Their Interligand Angles and the Synthesis and Characterization of a Monothiolato Pb(II) Bromide and Lithium Trithiolato Plumbate. *Inorg. Chem.* 2013, 52, 3054–3062.
- (34) Holligan, K.; Rogler, P.; Rehe, D.; Pamula, M.; Kornienko, A. Y.; Emge, T. J.; Krogh-Jespersen, K.; Brennan, J. G. Copper, Indium, Tin, and Lead Complexes with Fluorinated Selenolate Ligands: Precursors to MSe,. *Inorg. Chem.* **2015**, *54*, 8896–8904.
- (35) Kedarnath, G.; Kumbhare, L. B.; Dey, S.; Wadawale, A. P.; Jain, V. K.; Dey, G. K.  $\beta$ -Functionalized Ethylchalcogenolate Complexes of Lead(II): Synthesis, Structures and Their Conversion into Lead Chalcogenide Nanoparticles. *Polyhedron* **2009**, 28, 2749–2753.
- (36) Verma, A. K.; Rauchfuss, T. B.; Wilson, S. R. Donor Solvent Mediated Reactions of Elemental Zinc and Sulfur, sans Explosion. *Inorg. Chem.* **1995**, *34*, 3072–3078.
- (37) Kumar, R.; Mabrouk, H. E.; Tuck, D. G. Reactions of Some Main Group Metals with Diphenyl Disulphide and Diphenyl Diselenide. *J. Chem. Soc., Dalton Trans.* 1988, 1045–1047.

- (38) Dean, P. A. W.; Shrivastava, R. S. A Multinuclear, ( $^{77}$ Se,  $^{119}$ Sn,  $^{125}$ Te) Nuclear Magnetic Resonance Spectroscopic Study of the Series Sn(SPh)<sub>x</sub>(SePh)<sub>y</sub>(TePh)<sub>4-x-y</sub>. *Inorg. Chim. Acta* **1985**, *105*, 1–7. (39) Lowe, D. Science Translational Medicine. https://blogs.
- (39) Lowe, D. Science Translational Medicine. https://blogs.sciencemag.org/pipeline/archives/2012/05/15/things\_i\_wont\_work\_with\_selenophenol. (accessed December 21, 2019) Things I Won't Work With: Selenophenol.
- (40) Schroeder, T. B.; Job, C.; Brown, M. F.; Glass, R. S. Indirect Detection of Selenium-77 in Nuclear Magnetic Resonance Spectra of Organoselenium Compounds. *Magn. Reson. Chem.* **1995**, 33, 191–195
- (41) APEX2, version 2014.11-0; Bruker-AXS, 2014.
- (42) Sheldrick, G. M. Crystal Structure Refinement with SHELXL. Acta Crystallogr., Sect. C: Struct. Chem. 2015, 71, 3–8.
- (43) Sheldrick, G. M. SHELXT Integrated Space-Group and Crystal-Structure Determination. *Acta Crystallogr., Sect. A: Found. Adv.* **2015**, *71*, 3–8.